

The effect of high-fat feeding on intramuscular lipid and lipid peroxidation levels in UCP3-ablated mice

Joris Hoeks^{a,*}, Matthijs K.C. Hesselink^b, Wim Sluiter^c, Gert Schaart^b, Jodil Willems^a, Alastair Morrisson^d, John C. Clapham^{e,1}, Wim H.M. Saris^a, Patrick Schrauwen^a

^a Department of Human Biology, Nutrition and Toxicology Research Institute Maastricht (NUTRIM), Maastricht University, P.O. Box 616, 6200 MD Maastricht, The Netherlands

^b Department of Movement Sciences, Nutrition and Toxicology Research Institute Maastricht (NUTRIM), Maastricht University, P.O. Box 616, 6200 MD Maastricht, The Netherlands

^c Department of Biochemistry, Erasmus MC, Rotterdam, The Netherlands

^d Department of Comparative Genomics, GlaxoSmithKline, Harlow, Essex, United Kingdom

^e Department of Vascular Biology, GlaxoSmithKline, Harlow, Essex, United Kingdom

Received 5 December 2005; revised 11 January 2006; accepted 13 January 2006

Available online 26 January 2006

Edited by Barry Halliwell

Abstract Uncoupling protein-3 (UCP3) has been suggested to protect against lipid-induced oxidative damage. Therefore, we studied intramuscular lipid peroxide levels and high-fat diet induced alterations in muscle lipid metabolism of UCP3-ablated mice.

UCP3^{-/-} mice showed ~3-fold higher levels of intramuscular lipid peroxides upon standard chow feeding, compared to wild-type littermates. Remarkably, this difference was no longer apparent on the high-fat diet. However, upon high-fat feeding, intramuscular triacylglycerol levels were ~50% lower in UCP3^{-/-} mice, in comparison to UCP3^{+/+} animals. Succinate dehydrogenase activity, and total protein content of the muscle fatty acid transporter FAT/CD36 were however similar between UCP3^{-/-} and UCP3^{+/+} mice.

© 2006 Federation of European Biochemical Societies. Published by Elsevier B.V. All rights reserved.

Keywords: Mitochondrion; Lipotoxicity; Reactive oxygen species; UCP3; High fat diet

1. Introduction

Since the discovery of uncoupling protein-3 (UCP3) in 1997, many studies were devoted to the function of this UCP1 homologue, which is primarily expressed in skeletal muscle. However, its physiological role remains to be established. The most supported hypotheses concerning the physiological function of UCP3 state that this protein is either involved in the protection against reactive oxygen species (ROS) or has a role in fat metabolism. UCP3 is suggested to limit the production of ROS by mediating a mechanism of mild uncoupling resulting in a decrease in protonmotive force, thereby diminishing superoxide production [1]. Although there is support for a role of UCP3 in ROS defense [1–4], studies have also consistently

observed that UCP3 content is increased when the supply of lipids to the muscle exceeds the capacity to oxidize these lipids [5–9], and is decreased when fatty acid oxidation is improved [10,11] or lipid supply to the mitochondria is lowered [12]. Together, these data suggest that UCP3 may specifically have a function in the defense against excessive ROS production under conditions of high-fatty acid supply to the mitochondria. In that context, we previously hypothesized that UCP3 is involved in the outward translocation of non-metabolizable fatty acid anions, to protect mitochondria from the deleterious effects of intramitochondrial fatty acid accumulation [13]. When the fatty acid supply to the mitochondria exceeds the oxidative capacity, and the load of fatty acids on the mitochondrial membrane increases, neutral fatty acids can enter the inner mitochondrial membrane and reach the matrix side through flip-flop [14], where they will be deprotonated due to the proton gradient across the inner mitochondrial membrane. Because the mitochondrial membrane is impermeable to the resulting fatty acid anions [15], and because the fatty acids cannot be oxidized due to the lack of activation by acyl-CoA synthase, they are trapped at the matrix side of the inner mitochondrial membrane. Since the mitochondrial matrix is also the site where ROS is produced, these fatty acid anions are highly susceptible to peroxidation by the oxygen radicals. The resulting lipid peroxides are potentially hazardous to the mitochondrial proteins and DNA and could induce mitochondrial damage and dysfunction. By facilitating the export of these fatty acid anions, UCP3 could be involved in the protection of the mitochondria against lipid-induced oxidative damage. In a variant of this hypothesis, Goglia and Skulachev [16] suggested that UCP3 exports lipid peroxides, with the same protective function. Together with the anti-ROS hypothesis of the group of Brand [1,17], these three hypothesis all predict that a lack of UCP3 would result in lipid-induced oxidative damage.

In this context, insulin resistant subjects and type 2 diabetics are characterized by high fatty acid levels and low oxidative capacity, theoretically demanding a high UCP3 protein content to protect mitochondria against lipid-induced oxidative damage. Interestingly, however, type 2 diabetic patients are characterized by a 50% reduction in UCP3 protein content [18], increased levels of lipid peroxides [19] and mitochondrial

*Corresponding author. Fax: +31 0 43 3670976.
E-mail address: j.hoeks@hb.unimaas.nl (J. Hoeks).

¹ Present address: Department of Molecular Pharmacology, AstraZeneca R&D, Mölndal, Sweden.

damage and dysfunction [20–24]. It is therefore tempting to suggest that a low level of UCP3 fails to protect fatty acids against ROS-induced peroxidation, ultimately leading to lipid-induced mitochondrial damage in type 2 diabetic patients [25].

Therefore, we anticipated that lack of UCP3 would lead to increased levels of muscular lipid peroxides under diabetogenic conditions, such as on a high-fat diet and investigated the effect of UCP3 ablation on intramuscular lipid peroxide levels and high-fat diet induced alterations in muscle lipid metabolism.

2. Methods

2.1. Animals

Sixteen UCP3-ablated (aged: 12.2 ± 1.3 weeks) and 12 wild-type littermates (aged: 12.8 ± 1.2 weeks), original breeding pairs a gift from GlaxoSmithKline (Harlow, UK), were used in the present study [26]. The mice were housed individually on a 12:12 h light–dark cycle (light from 7:00 a.m. to 7:00 p.m.), at 21–22 °C and subjected to a four week–week dietary intervention. During the experiments, mice had free access to tap water. All experiments were approved by the Institutional Animal Care and Use Committee of the Maastricht University and complied with the principles of laboratory animal care.

2.2. Diets

UCP3 ablated mice (UCP3^{-/-}) and their wild-type littermates (UCP3^{+/+}) were randomly divided into a total of four groups. Eight UCP3^{-/-} and six UCP3^{+/+} mice had unlimited access to standard chow diet (ssniff® r/m-h 10 mm, Bio Services, Uden, The Netherlands, 16.3 MJ/kg, 7.5 EN% from fat) for the duration of four weeks. Another eight UCP3^{-/-} and six UCP3^{+/+} mice were maintained on a high-fat diet (4031.10, Hope Farms, Woerden, The Netherlands, 19.8 MJ/kg, 45 EN% from fat), which was also provided ad libitum. In the high-fat diet, the fat component was comprised of C16:0 (~25%), C18:0 (~34%), C18:1 (~33%), C18:2 (~3%) and C24:0 (~5%). Food intake and body mass were recorded.

2.3. Tissue sampling

After the four-week dietary intervention period, tissue dissection was performed under general anesthesia (1.5–2.0% halothane in O₂ and N₂O [3:1, 4.0 l/min]). Mice were deprived from food approximately 8 h prior to tissue sampling. For histological analysis, the mid-belly region of the left tibialis anterior muscle was dissected and freed from any visible fat and blood, embedded in Tissue-Tek (Sakura Finetek, Zoeterwoude, The Netherlands) and rapidly frozen in liquid nitrogen-cooled isopentane (2-methyl-butane, Fluka, Zwijndrecht, The Netherlands). The tibialis anterior muscle of the contralateral leg was dissected and immediately frozen in liquid nitrogen for the determination of lipid hydroperoxide (LPO) levels. All samples were stored at –80 °C until further analysis.

2.4. Determination of intramuscular LPO

Snap-frozen tissues in liquid nitrogen were pulverized during three min at 1800 rpm in a Braun Mikro-dismembrator homogeniser type U (Braun Biotech Int., Melsungen, Germany) using a PTFE-coated steel bead of 10 mm in diameter, next suspended 1:3 (wt/vol) in phosphate-buffered saline, pH

7.4, supplemented with 4 mM butylated hydroxytoluene and further homogenized at 4 °C using a Teflon hand-held pestle in an Eppendorf vial. The concentration of LPO of the homogenate was determined after incubation with 35 U/ml catalase for two min at room temperature to inactivate any hydrogen peroxide, by the ferric iron-dependent increase in absorbance of xylenol-orange at 560 nm (LPO apparent $\epsilon = 0.08904 \mu\text{M}^{-1} \text{cm}^{-1}$, experimentally assessed using freshly-made reagents only and standard curves of *t*-butyl peroxide and cumene peroxide) essentially as described by Nourooz-Zadeh et al. [27] using the sample treated by 0.9 mM tris(2-carboxyethyl)phosphine to reduce the LPO to their respective alcohols as the reference.

2.5. Histological analysis

Cryosections (5 μm) were thaw mounted on uncoated pre-cleaned (96% ethanol) glass slides. Immediately after mounting, air-dried, fresh cryosections were stained for intramuscular triacylglycerols (IMTG) by Oil Red O staining (ORO) [28] combined with immunolabeling of the basal membrane marker laminin, to allow quantification of IMTG. Serial sections were stained for activity of succinate dehydrogenase (SDH), also known as complex II in the electron transport chain, to determine the oxidative capacity of skeletal muscle, largely according to [29].

2.6. IMTG analysis

Briefly, cryosections were fixed in 3.7% formaldehyde for 1 h. Then the sections were treated with 0.5% Triton X-100 in PBS for 5 min, and washed three times with PBS. Thereafter, sections were incubated for 30 min with a polyclonal rabbit antibody against the basement membrane protein laminin (Sigma–Aldrich, St. Louis, MO, USA, 1:50 dilution in PBS) to visualize individual cell membranes followed by a 30 min incubation with a FITC-conjugated goat anti-rabbit (Southern Biotechnologies Associates, ITK, Uithoorn, The Netherlands; 1:80 dilution in PBS). After washing with PBS, glass slides were immersed in the ORO working solution for 30 min for the detection of lipid droplets (17) and rinsed three times with deionized water for 30 s followed by 10 min of washing with running tap water. Stained sections were embedded in Mowiol.

2.7. SDH activity analysis

Cryosections were incubated in a 0.2 M sodium phosphate buffer containing 0.1 M succinic acid (Sigma–Aldrich) and 1.2 mM nitro-blue tetrazolium (Sigma–Aldrich). Incubation was performed at a strictly controlled temperature of 37 °C for the duration of 60 min. Next, sections were shortly rinsed with deionized water followed by three successive exchanges in 30%, 60% and 90% acetone in deionized water, respectively. SDH-stained sections were air-dried for 15 min. Thereafter, also these sections were incubated for 30 min with the laminin-antibody and the FITC-conjugated secondary antibody, respectively, to visualize the cell membranes. Stained sections were embedded in Mowiol. Following this procedure sites of high SDH activity are colored gray-blue whereas low SDH activity results in a pale color [29].

2.8. Image capturing, processing, and analysis

All sections were examined using a Nikon E800 fluorescence microscope (Nikon Instruments Europe B.V., Badhoevedorp,

The Netherlands) coupled to a Basler A101C progressive scan color charge-coupled device camera. Multiple random images were captured for every single color (red and green) in case of the ORO and in bright field for the SDH activity staining. The fluorescent signal representing the cellular membrane in the SDH stained sections was grabbed in the appropriate channel and SDH activity was imaged using bright field. Both images, as well as the merged overlay were saved. All sections were processed and analyzed using Lucia GF 4.80 software (Nikon, Düsseldorf, Germany). Special care was taken to use the same camera settings (gain and exposure time, and voltage and diaphragm in case of bright field) while grabbing all images. For both SDH and IMTG >120 cells per muscle were analyzed.

2.9. IMTG

All images were analyzed for the lipid droplet over myocyte area fraction. To this end, a semiautomatic macro was written that allowed: (1) autodetection of the cellular membrane (identified in the green channel); (2) measurement of the area covered by the measured myocytes; and (3) measurement of the area covered by lipid droplets (identified in the red channel). The area fraction was computed by dividing the area covered by lipid droplets (in μm^2) by the cell surface of the measured myocytes (in μm^2). The mean area fraction thus reflects the percentage of the total measured cell surface covered by lipid droplets.

2.10. SDH activity

Like in the IMTG analyses, a semiautomatic macro was used to identify the cellular membrane. The bright-field image of SDH activity was converted to 8-bits grayscale after which integral optical density of every pixel in individual muscle cells was measured. The mean optical density of every individual cell was computed and used as a semi-quantitative read-out for SDH activity. Similar methods have previously been shown to correlate well with whole muscle homogenate spectrophotometrical analysis of SDH activity [30,31].

2.11. Western blot analysis of FAT/CD36

Muscle homogenates were analyzed for the muscle fatty acid transporter FAT/CD36 by Western blotting according to the procedure described by Keizer et al. [32]. After electrophoresis and blotting, nitrocellulose membranes were blocked for 20 min with 5% non-fat dried milk in 0.05% Tween 20/PBS and incubated with a mouse IgA monoclonal antibody raised against mouse FAT/CD36 (MAB1258-Chemicon, Invitrogen, Breda, The Netherlands) 1:10000 in blocking buffer. After the primary antibody incubation, the membranes were incubated for 60 min with a horseradish peroxidase-conjugated rabbit anti-mouse IgA (Southern Biotechnology Associates, ITK, Uithoorn, The Netherlands) at a dilution of 1:5000 in blocking buffer. The membranes were then washed for 1.5 h in 0.05% Tween 20/PBS and again for 10 min in PBS. Subsequently, they were treated for 1 min with enhanced chemiluminescence substrate (Super Signal West Dura Extended Duration Substrate; Pierce/Perbio Science, Etten-Leur, The Netherlands). Finally, nitrocellulose membranes were exposed to X-ray film (CL-Xposure Film; Pierce/Perbio Science) for 1 min and analyzed by densitometry using Imagemaster (Pharmacia Biotech).

2.12. Statistical analysis

Results are presented as means \pm S.E.M. Differences within animals were analyzed by the Wilcoxon signed-rank test for paired samples. Differences between genotypes were evaluated by the Mann–Whitney test for independent samples. Outcomes were regarded as statistically significant if $P < 0.05$.

3. Results

3.1. Body mass and food intake

Initial body mass in the chow group was not statistically different between genotypes (20.6 ± 1.0 vs. 24.6 ± 1.9 g in UCP3^{-/-} and UCP3^{+/+} mice, respectively, $P = 0.14$). Four weeks of chow feeding did not change body mass, neither in UCP3^{-/-} nor in UCP3^{+/+} animals (by 0.3 ± 0.6 vs. -0.5 ± 1.1 g in UCP3^{-/-} and UCP3^{+/+} animals, respectively, NS). Gross energy intake during four weeks of chow feeding was significantly lower in UCP3^{-/-} animals, compared to their wild-type littermates (1693 ± 63 vs. 1874 ± 47 kJ/4 weeks, $P = 0.043$). The gross energy intake positively correlated with initial body mass ($r = 0.53$; $P = 0.052$) and when expressed per gram of initial body mass, gross energy intake was not significantly different between the groups (UCP3^{-/-}: 82.9 ± 3.5 ; UCP3^{+/+}: 78.6 ± 6.2 kJ/g/4 weeks, $P = 0.49$, NS).

Initial body mass in the HF group was similar between UCP3^{-/-} and UCP3^{+/+} mice (21.4 ± 1.4 vs. 24.4 ± 1.8 g, respectively, $P = 0.18$). Four weeks of HF feeding significantly increased body mass in both genotypes (by 1.6 ± 0.4 g [$P = 0.012$] in UCP3^{-/-} and by 2.4 ± 1.0 g [$P = 0.046$] in UCP3^{+/+}). The increase in body mass upon HF feeding, was not different between the two genotypes ($P = 0.76$). Gross energy intake upon HF diet was comparable in UCP3^{-/-} and UCP3^{+/+} mice (1929 ± 82 vs. 2189 ± 107 kJ/4 weeks, respectively, $P = 0.11$), and correlated with initial body mass ($r = 0.74$; $P = 0.002$). Gross energy intake per gram of initial body mass was similar between genotypes (UCP3^{-/-}: 91.7 ± 4.0 ; UCP3^{+/+}: 91.6 ± 6.1 kJ/g/4 weeks, $P = 0.85$, NS).

3.2. Intramuscular LPO and triacylglycerol levels

UCP3^{-/-} animals ($n = 8$) showed significantly higher levels of intramuscular LPO upon chow feeding, as compared to UCP3^{+/+} ($n = 6$) mice (38.2 ± 11.2 vs. 12.5 ± 0.9 nmol/g wet weight, $P = 0.001$). Surprisingly, 4 weeks of high-fat feeding resulted in similar LPO levels in UCP3^{-/-} vs. UCP3^{+/+} mice (13.6 ± 3.2 [$n = 8$] vs. 16.2 ± 5.1 nmol/g wet weight [$n = 6$], respectively, $P = 0.85$, NS; Fig. 1).

Upon chow feeding, no differences in IMTG levels (Fig. 2) were found between UCP3^{-/-} ($n = 8$) and UCP3^{+/+} ($n = 6$) animals ($0.68 \pm 0.44\%$ vs. $0.72 \pm 0.32\%$ of the cell surface covered by lipid droplets, respectively, $P = 0.70$, NS). After four weeks of HF diet, IMTG levels were significantly lower in the UCP3^{-/-} ($n = 8$) animals compared to their wild-type ($n = 5$) littermates ($1.39 \pm 0.44\%$ vs. $3.01 \pm 0.35\%$, respectively, $P = 0.019$).

3.3. Oxidative capacity

Oxidative capacity, measured as SDH activity, was similar in UCP3^{-/-} and UCP3^{+/+} mice, after chow (UCP3^{-/-}: 0.32 ± 0.05 [$n = 7$] vs. UCP3^{+/+}: 0.31 ± 0.06 AU [$n = 4$]) as well

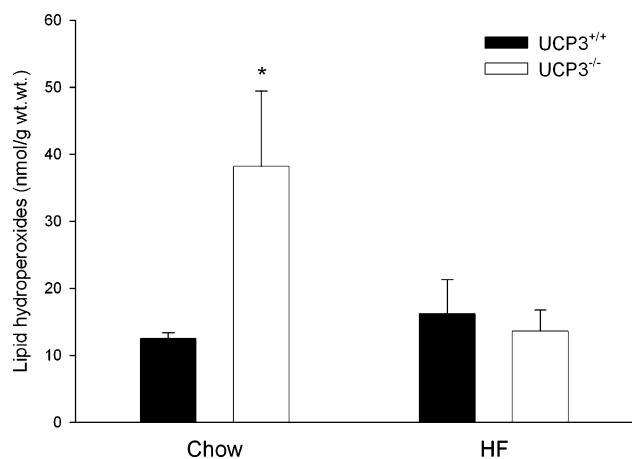


Fig. 1. Intramuscular LPO levels in m. tibialis anterior upon chow and high-fat (HF) feeding. * $P < 0.05$ compared to UCP3^{+/+} upon chow feeding.

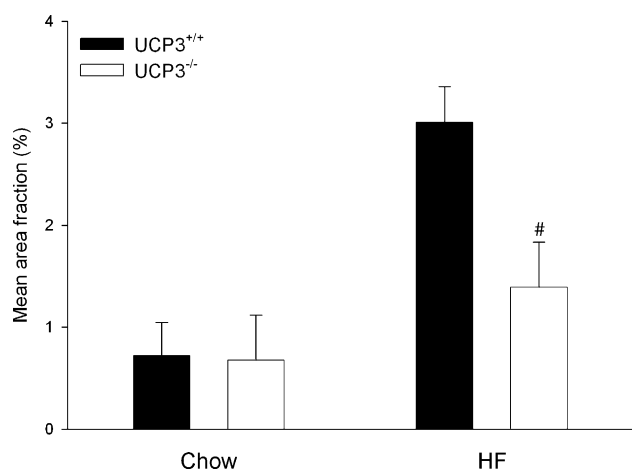


Fig. 2. IMTG levels in m. tibialis anterior after 4 weeks of chow or high-fat (HF) feeding. # $P < 0.05$ compared to UCP3^{+/+} upon HF feeding.

as after HF feeding (UCP3^{-/-}: 0.36 ± 0.08 [$n = 7$] vs. UCP3^{+/+}: 0.39 ± 0.06 AU [$n = 5$]).

3.4. Fatty acid transporter FAT/CD36

Protein levels of FAT/CD36, determined by Western blotting, were similar between UCP3^{-/-} ($n = 4$) and UCP3^{+/+} ($n = 5$) mice after chow feeding and averaged 124 ± 25 and 101 ± 24 AU, respectively. Also after 4 weeks of high-fat diet, no significant differences were detected between UCP3^{-/-} (73 ± 19 AU, $n = 8$) and UCP3^{+/+} (86 ± 13 AU, $n = 5$) mice.

4. Discussion

The physiological function of UCP3 is still under debate. However, several lines of evidence point towards a role for this mitochondrial protein in protection against lipid-induced oxidative damage to mitochondria. We have previously hypothesized that UCP3 fulfils this protective role in skeletal muscle

mitochondria by exporting non-metabolizable fatty acid anions away from the side of the mitochondrial matrix, a function especially important in situations of increased lipid supply. ROS, regarded as inevitable by-products of normal aerobic metabolism, can peroxidize these fatty acid anions, giving rise to toxic and highly reactive lipid peroxides that would be trapped in the inner mitochondrial membrane and/or matrix. In addition to this putative role of UCP3, it has also been hypothesized that UCP3, upon activation by lipid peroxides (such as 4-hydroxy-*trans*-2-nonenal, 4HNE), reduces ROS production directly [1,3,17]. Indeed, Echay et al. [1] showed that 4HNE was able to uncouple skeletal muscle mitochondria in the absence, but not in the presence of GDP, indicative of UCP-mediated uncoupling. Moreover, the uncoupling effect of 4HNE was significantly less in UCP3-ablated mice compared to wild-type mitochondria [1]. Furthermore, GDP did not prevent the stimulation of proton conductance in UCP3 ablated mice. Thus, the increased UCP3 activity upon lipid peroxides, such as 4HNE, lowers protonmotive force and results in a decrease in superoxide production, thereby providing a simple feedback loop [17].

However, according to both hypotheses, UCP3 ablation would lead to increased levels of lipid peroxides, especially during lipid oversupply. Here we show that UCP3-ablated mice display significantly higher levels of intramuscular LPO upon standard chow feeding. Surprisingly, however, no increase in lipid peroxidation in UCP3^{-/-} mice was observed on a high-fat diet, but under this condition, other adaptive mechanisms seem to operate preventing further augmentation of intramuscular lipid peroxides.

In addition to confirm the previous finding that levels of lipid peroxides are increased in UCP3^{-/-} mice on a chow diet [2], the present study remarkably showed that, UCP3^{-/-} mice did not differ in their levels of lipid peroxides upon a high-fat diet, as would have been expected on the basis of the present hypotheses on the physiological function of UCP3. This may indicate that UCP3 is not important in the prevention of ROS production under high-fat conditions. More likely, however, UCP3^{-/-} animals may display other protective mechanisms to cope with the increased lipid supply and/or increased ROS production. To elucidate that, we examined whether UCP3^{-/-} mice on a high fat diet were able to limit the storage of muscular fatty acids. To this end, we measured IMTG levels by ORO staining in UCP3^{-/-} and UCP3^{+/+} mice, both after chow and high-fat feeding. Surprisingly, UCP3^{-/-} mice were indeed characterized by markedly lower IMTG levels (~54%) compared to their wild-type littermates upon 4 weeks of high-fat diet.

The difference in lipid peroxidation between UCP3^{-/-} and UCP3^{+/+} mice upon chow feeding, would be maintained ($P = 0.06$) under high-fat conditions if the muscular lipid peroxidation is expressed per unit of muscular lipid. However, our data clearly illustrate that this is not directly due to the lack of protection by UCP3, but due to a remarkable lowering of the amount of intramuscular lipids. In fact, IMTG levels in UCP3^{-/-} mice fed a high-fat diet were only marginally higher compared to chow-fed UCP3^{-/-} mice, whereas in wild-type animals, 4 weeks of HF diet caused a ~4.4-fold increase in IMTG levels. These differences could not be accounted for by differences in muscle fiber type distribution (data not shown). A reduction in IMTG levels can, based on the putative functions of UCP3, not be directly deduced from the lack of

UCP3 and it is therefore tempting to speculate that the reduction in IMTG represents an adaptive mechanism to limit peroxidation of muscular fatty acids by the increased ROS production that has been observed in muscle of UCP3^{-/-} mice on a regular diet [2,4].

To address the question how UCP3^{-/-} mice are capable of limiting intramuscular fat accumulation upon a high-fat diet, we examined oxidative capacity in these mice. However, we could not detect any differences in oxidative capacity between UCP3^{-/-} and UCP3^{+/+} mice, neither on a chow nor on a high-fat diet. These results are compatible with the finding that UCP3 ablation on a chow diet had no effect on markers of fatty acid oxidation [33], as well as with the results of Vidal-Puig et al. [4] who were unable to show a difference in fatty acid oxidation between UCP3^{-/-} and UCP3^{+/+} mice, neither in sedentary nor in exercised animals. Moreover, in the fasted state an impaired, in contrast to improved, fat oxidation in UCP3^{-/-} mice was observed [34].

Vidal-Puig et al. [4] reported earlier that UCP3^{-/-} mice display increased plasma free fatty acid levels, when challenged with a high-fat diet. This finding indicates that the lower IMTG levels that we observed in UCP3^{-/-} mice upon high-fat feeding, cannot be explained by a diminished supply of fatty acids to the muscle, but is suggestive for a decreased fat uptake in muscle. To this end, we determined protein levels of the muscle fatty acid transporter, FAT/CD36, which has been shown to be involved in the uptake of plasma free fatty acids into skeletal muscle. Nevertheless, we could not detect any differences in the protein levels of FAT/CD36 between UCP3^{-/-} and UCP3^{+/+} mice. However, controlled measurements with labeled fatty acids may be required to exclude the possibility of diminished fatty acid uptake in skeletal muscle from UCP3^{-/-} mice upon high-fat feeding.

In summary, UCP3^{-/-} mice show significantly higher levels of intramuscular lipid peroxides upon standard chow feeding, as compared to their wild-type littermates. Remarkably however, no differences were observed in the levels of lipid peroxides after 4 weeks of a HF diet. The latter observation was accompanied by the finding that, upon HF feeding, IMTG levels were markedly lower in UCP3^{-/-} mice, in comparison to the UCP3^{+/+} animals. Differences in oxidative capacity, as assessed by SDH activity, or the protein levels of FAT/CD36 could not account for the lower IMTG levels, observed in UCP3-ablated mice on a HF diet. Therefore, the exact underlying (molecular) mechanism for the reduced IMTG levels in UCP3^{-/-} mice remains to be established.

These data also indicate that the UCP3^{-/-} mouse may not be the best model to answer the question whether low UCP3 levels will lead to lipid-induced mitochondrial damage and contribute to the pathogenesis of type 2 diabetes, as we have previously suggested [25]. Such information, however, is eagerly awaited since insulin resistant subjects and/or type 2 diabetic patients are characterized by a 50% reduction of UCP3 protein content [18] and are also characterized by increased levels of lipid peroxidation [19] and mitochondrial damage [20], but may require novel methodologies such as siRNA to acutely suppress UCP3. The adaptive capacity to reduce IMTG levels in UCP3^{-/-} mice may also explain why these mice have no apparent phenotype (such as obesity and diabetes).

Acknowledgements: MSc. J. Hoeks was supported by a grant from the Netherlands Organization for Scientific Research (NWO) and the research of Dr. P. Schrauwen has been made possible by a fellowship of the Royal Netherlands Academy of Arts and Sciences.

References

- [1] Echtay, K.S. et al. (2003) *EMBO J.* 22, 4103–4110.
- [2] Brand, M.D., Pamplona, R., Portero-Otin, M., Requena, J.R., Roebuck, S.J., Buckingham, J.A., Clapham, J.C. and Cadenas, S. (2002) *Biochem. J.* 368, 597–603.
- [3] Echtay, K.S. et al. (2002) *Nature* 415, 96–99.
- [4] Vidal-Puig, A.J. et al. (2000) *J. Biol. Chem.* 275, 16258–16266.
- [5] Schrauwen, P. et al. (2003) *FASEB J.* 17, 2272–2274.
- [6] Schrauwen, P., Hinderling, V., Hesselink, M.K., Schaart, G., Kornips, E., Saris, W.H., Westerterp-Plantenga, M. and Langhans, W. (2002) *FASEB J.* 16, 1688–1690.
- [7] Schrauwen, P., Hoppeler, H., Billeter, R., Bakker, A.H. and Pendergast, D.R. (2001) *Int. J. Obes. Relat. Metab. Disord.* 25, 449–456.
- [8] Hoeks, J., Hesselink, M.K., van Bilsen, M., Schaart, G., van der Vusse, G.J., Saris, W.H. and Schrauwen, P. (2003) *FEBS Lett.* 555, 631–637.
- [9] Hesselink, M.K. et al. (2001) *FASEB J.* 15, 1071–1073.
- [10] Russell, A.P. et al. (2003) *J. Physiol.* 550, 855–861.
- [11] Schrauwen, P., Schaart, G., Saris, W.H., Sliker, L.J., Glatz, J.F., Vidal, H. and Blaak, E.E. (2000) *Diabetologia* 43, 1408–1416.
- [12] Hoeks, J., van Baak, M.A., Hesselink, M.K., Hul, G.B., Vidal, H., Saris, W.H. and Schrauwen, P. (2003) *Am. J. Physiol. Endocrinol. Metab.* 285, E775–E782.
- [13] Schrauwen, P., Saris, W.H. and Hesselink, M.K. (2001) *FASEB J.* 15, 2497–2502.
- [14] Hamilton, J.A. and Kamp, F. (1999) *Diabetes* 48, 2255–2269.
- [15] Jezek, P., Orosz, D.E., Modriansky, M. and Garlid, K.D. (1994) *J. Biol. Chem.* 269, 26184–26190.
- [16] Goglia, F. and Skulachev, V.P. (2003) *FASEB J.* 17, 1585–1591.
- [17] Brand, M.D. et al. (2004) *Biochem. Soc. Symp.*, 203–213.
- [18] Schrauwen, P., Hesselink, M.K., Blaak, E.E., Borghouts, L.B., Schaart, G., Saris, W.H. and Keizer, H.A. (2001) *Diabetes* 50, 2870–2873.
- [19] Russell, A.P. et al. (2003) *FEBS Lett.* 551, 104–106.
- [20] Kelley, D.E., He, J., Menshikova, E.V. and Ritov, V.B. (2002) *Diabetes* 51, 2944–2950.
- [21] Mootha, V.K. et al. (2003) *Nat. Genet.* 34, 267–273.
- [22] Patti, M.E. et al. (2003) *Proc. Natl. Acad. Sci. USA* 100, 8466–8471.
- [23] Petersen, K.F. et al. (2003) *Science* 300, 1140–1142.
- [24] Petersen, K.F., Dufour, S., Befroy, D., Garcia, R. and Shulman, G.I. (2004) *N. Engl. J. Med.* 350, 664–671.
- [25] Schrauwen, P. and Hesselink, M.K. (2004) *Diabetes* 53, 1412–1417.
- [26] Cadenas, S. et al. (2002) *J. Biol. Chem.* 277, 2773–2778.
- [27] Nourooz-Zadeh, J., Tajaddini-Sarmadi, J. and Wolff, S.P. (1994) *Anal. Biochem.* 220, 403–409.
- [28] Koopman, R., Schaart, G. and Hesselink, M.K. (2001) *Histochem. Cell Biol.* 116, 63–68.
- [29] Sheehan, D.C. and Hrapchak, B.B. (1987) *Theory and Practice of Histotechnology*, Batelle Press, Ohio.
- [30] Skorjanc, D., Heine, G. and Pette, D. (1997) *Histochem. Cell Biol.* 107, 47–55.
- [31] Martin, T.P., Vailas, A.C., Durivage, J.B., Edgerton, V.R. and Castleman, K.R. (1985) *J. Histochem. Cytochem.* 33, 1053–1059.
- [32] Keizer, H.A., Schaart, G., Tandon, N.N., Glatz, J.F. and Luiken, J.J. (2004) *Histochem. Cell Biol.* 121, 101–107.
- [33] Bezaire, V., Spriet, L.L., Campbell, S., Sabet, N., Gerrits, M., Bonen, A. and Harper, M.E. (2005) *FASEB J.*
- [34] Bezaire, V., Hofmann, W., Kramer, J.K., Kozak, L.P. and Harper, M.E. (2001) *Am. J. Physiol. Endocrinol. Metab.* 281, E975–E982.